IN -64- TM

5339

P- 14

Aerospace Applications of Integer and Combinatorial Optimization

by

S. L. Padula
NASA Langley Research Center
Hampton, VA

and
R. K. Kincaid
Department of Mathematics
College of William and Mary
Williamsburg, VA

Abstract

Research supported by NASA Langley Research Center includes many applications of aerospace design optimization and is conducted by teams of applied mathematicians and aerospace engineers. This paper investigates the benefits from this combined expertise in formulating and solving integer and combinatorial optimization problems. Applications range from the design of large space antennas to interior noise control. A typical problem, for example, seeks the optimal locations for vibration-damping devices on an orbiting platform and is expressed as a mixed/integer linear programming problem with more than 1500 design variables.

Introduction

The purpose of this effort is to investigate the interchange of ideas between aerospace engineers and applied mathematicians in formulating and solving design optimization problems. This research also describes and provides examples of integer and combinatorial optimization applications that have been studied at NASA Langley Research Center.

Several optimization methods, including simulated annealing, tabu search and branch and bound, for solving combinatorial optimization problems are mentioned herein. These are heuristic (i.e., rule-based) methods and are not guaranteed to converge to a global minimum. A brief characterization of each method is given below. For a detailed description, the interested reader is referred to the appropriate references.

Metaheuristics such as simulated annealing and tabu search provide a shell within which a variety of other heuristics may be implemented. The definitions and notations that follow are taken from references 1-3.

Let Σ denote the set of all feasible states (i.e., the set of feasible solutions to the minimization problem generated from all possible combinations of the design variables) and let S denote an element of Σ. To differentiate between states we define a criterion function c and refer to $c(S)$ as the cost of state S. To move from one state to another we define a move set Δ and a move $\delta \in \Delta$. The outcome of applying all legal moves $\delta \in \Delta$ to the current state S defines the set of states reachable from S; this set is typically called the neighborhood of S. The value of a move is the difference between the cost of the new state and the cost of S (i.e., $c[\delta(S)] - c(S)$).

Each metaheuristic begins with an initial state S_0, chosen either at random or constructed algorithmically. Then the metaheuristic generates a sequence of moves $\{\delta_0, \delta_1, ..., \delta_n\}$ which determines a sequence of states through which the search proceeds.

The mechanism by which a move is selected is one of the crucial differences between simulated annealing and tabu search. To appreciate the difference consider an improvement scheme that at state S_t selects the greatest available one-move improvement. That is, the next move δ_t is chosen based on minimum cost:

$$c[\delta_t(S_t)] = \min_{\delta \in \Delta} c[\delta(S_t)] \qquad (1)$$

Equation (1) is called a greedy local improvement scheme and a metaheuristic based on equation (1) is called a greedy search algorithm. The greedy search terminates when no improving move is found. The final state of a greedy search is a local minimum (with respect to a particular move structure) and is, generally, not the global minimum. Both simulated annealing and tabu search are attempts to circumvent this difficulty. In simulated annealing nonimproving moves are initially accepted with a high probability; the probability is gradually decreased. Simple versions of tabu search attempt to avoid entrapment in local minima by maintaining a list of previously selected moves and deleting them from the move set Δ for a state S to avoid a return to a previously observed state. More sophisticated features of tabu search involve explicit use of the search history to diversify or intensify the search.

The branch and bound algorithm with linear programming (LP) relaxations (e.g., see ref. 4) is an alternative to the above heuristic algorithms. This technique is a good choice for combinatorial optimization problems that involve binary design variables and linear criterion functions and linear constraints. The method solves a sequence of LP problems that establish upper and lower bounds on the solution to the integer linear programming (ILP) problem. These bounds are used to "prune" branches from the binary tree which describes the state space Σ. The method terminates after a fixed number of LP problems have been considered or when the difference between the newest upper and lower bounds is small compared with the modeling or measurement uncertainty.

Three aerospace integer or combinatorial optimization problems are cited in this paper. The first involves the selection of the best assembly sequence for a large space antenna; the second seeks optimal locations for vibration-damping devices on an orbiting space platform; and the third involves determination of the number and position of active structural acoustic control actuators. For each case, the mathematical problem statement is

given, a solution method is suggested, and typical results are examined. Moreover, the contributions of mathematicians and engineers to the solution of the problem are acknowledged; and obstacles encountered in the solution process are reviewed.

Antenna Assembly Sequence Problem

Assume that an antenna (fig. 1(a)) is to be designed and erected in space using a large number n of truss elements. For research purposes, the antenna structure is designed as a tetrahedral truss (fig. 1(b)) with a flat top surface (i.e., all nodes in the top surface of the finite-element model are coplanar). The lengths of the truss elements must be identical to minimize surface distortion and to avoid the buildup of internal forces during the assembly process. However, because of unavoidable manufacturing limitations, the lengths are never precisely identical. Each truss element j has a small but measurable error e_j. One way to minimize the impact of these errors is to assemble the antenna in such a way that the errors offset one another.

A combinatorial optimization problem that determines the best arrangement of the truss elements is developed here. First, the objective is stated as the minimization of the squared L_2 norm of the surface distortion:

$$d^2 = e^T U^T D U e = e^T H e \qquad (2)$$

where e is the vector of measured errors; U is the influence matrix such that u_{ij} gives the influence of a unit error in member j on the surface distortion at node i; and D is a positive semidefinite weighting matrix that denotes the relative importance of each node i at which distortion is measured. The matrix U can be calculated by any structural analysis software package, and the matrix D is often the identity matrix. With these definitions, the antenna distortion problem is stated as

$$\text{minimize} \quad \sum_{j=1}^{n} \sum_{i=1}^{n} e_i h_{ij} e_j \qquad (3)$$

over all permutations of the error vector e. Clearly equation (3) is a quadratic assignment problem; however this equation is not the typical version studied in the operations research literature.

For the antenna assembly sequence problem, engineering insight led directly to a mathematical solution process. The authors of reference 5 observe that the cost of truss elements increases dramatically when unusual precision in length is demanded. They

suggest that truss elements with standard precision would be adequate if assembled in the correct order. Because construction of the antenna in space requires careful planning of the assembly sequence, the mathematical assignment of truss elements to specific antenna locations does not increase the complexity of the process.

In reference 5 the following conceptual solution is proposed. The antenna is assembled with a random assignment of elements. Pairs of elements are selected at random and interchanged. If the surface distortion degrades then the interchange is reversed, otherwise it remains. This process continues until no further improvement is realized. The effect of interchanges can be predicted using equation (2) so that no hardware changes must be made until the best arrangement has been identified (ref. 5).

The pairwise interchange heuristic that is suggested in reference 5 is similar to the greedy heuristic discussed in the introduction. This interchange heuristic is inferior to the simulated annealing or tabu search algorithms developed in references 6-7. For example, Figure 2 shows a comparison of the simulated annealing results with those of the pairwise interchange. In each trial both methods are initialized with the same random assembly sequence and the results of ten trials are plotted. Both methods result in final assembly sequences which are orders of magnitude better than the initial random sequence. However, the simulated annealing method consistently results in an excellent solution, and the pairwise interchange usually converges to an inferior solution.

Suggestions from aerospace engineers for the antenna assembly sequence problem led directly to a good problem formulation and to a workable combinatorial optimization scheme. Applied mathematicians suggested an improved optimization scheme. The next two case studies suggest that formulating the correct optimization problem generally requires more interaction between mathematicians and engineers.

Damper Placement Problem (DPP)

One aspect of the NASA Controls-Structures Interaction (CSI) project was a set of laboratory experiments investigating the control of space structures. The Phase 1 CSI Evolutionary Model (CEM) was a large, flexible structure assembled from truss elements and antenna support members. (See fig. 3.) The CEM was designed to simulate some characteristics of a large earth-observation platform. The CEM was suspended by cables and was dynamically tested in the NASA Langley Space Structures laboratory. After the dynamic characteristics of the original model were measured, numerous active control concepts were applied and tested.

In one active control concept (ref. 8), 8 of the 1507 truss elements were removed and replaced by active struts. An active strut is a combination of an actuator and a sensor. Active struts can sense axial compression or tension and use a feedback control law to dissipate strain. Active struts that are placed in high-strain locations can enhance vibration damping.

The goal of the DPP is to determine optimal locations for 8 active struts so as to maximize the minimum modal damping ratio over the first 26 characteristic vibration modes of the structure. As explained in reference 8, the goal is to improve damping in all target modes so that any vibration induced in the structure will decay quickly. In reference 8, the DPP is expressed as a mixed ILP problem with 1508 design variables and 27 constraints:

$$\text{maximize} \quad \beta$$
$$\text{such that} \quad \sum_j v_{ij} x_j \geq w_i \beta \quad \text{for i} = 1, 2, ...26$$
$$\text{and} \quad \sum_j x_j \leq 8 \tag{4}$$
$$\text{design variables}: \quad \beta, x_1, ..., x_{1507}$$

where v_{ij} is the fraction of axial strain energy in mode i and truss element j; β is a real-valued design variable that is proportional to the minimum modal damping ratio; and x is a vector of binary design variables such that $x_j = 1$ if truss element j is to be replaced. The optional vector of weighting factors w can be used if the control of certain modes is particularly important.

For this second case study, engineering insight led to a useful description of the physical problem but did not provide an effective mathematical solution method. One possible solution method is to select the location j with the maximum value of v_{ij} for each mode i. This method is reasonable for controlling one or two modes. However, if 8 struts must provide damping for 26 modes, then locations that simultaneously provide damping in several different modes must be sought.

Reference 9 contains information used to describe and formulate the DPP. The authors suggest the use of the sum of axial strain energy ($\sum v_{ij} x_j$) as a measure of damping in mode i. In addition, they suggest that the weights should be proportional to the percent of modal damping in mode i (i.e., $w_i \propto \sum_j v_{ij}$). This insight is important because many of the first 26 modes in the CEM involve motion of suspension cables and deformation of the antenna support elements. The sum of modal strain energy due to tension or compression of the truss elements is tiny for such modes. Modes that cause little

or no strain in the truss elements cannot be controlled by placing active struts in truss locations. This phenomenon suggests that $w_i = 0$ if the modal strain energy is small (e.g., less than 30 percent) and $w_i = 1$ otherwise.

Reference 9 provides relevant information in regard to the physics of the DPP but does not provide efficient solution techniques. Instead of stating the problem as in equation (4), the authors pose the following unconstrained nonlinear programming problem:

$$\max \left\{ \frac{1}{26} \sum_{i=1}^{26} \left[\sum_{j=1}^{1507} \left(x_j v_{ij} \Big/ \zeta_i \right) \right]^{1/4} \right\}^4 \tag{5}$$

design variables : x_j

where ζ_i is a target value of damping in mode i. The solution method is simulated annealing.

Equation (4) is preferred over equation (5) for three practical reasons. First, equation (5) will not necessarily provide damping in each controllable mode. Second, no straightforward method exists for adding topological constraints to equation (5). Third, the effort required to solve equation (5) by simulated annealing increases with the size of the search domain:

$$\text{size} = \frac{N!}{\left[M!(N-M)! \right]} \tag{6}$$

where $N = 1507$ is the number of possible locations and $M = 8$ is the number of active struts. The number of combinations of 1507 locations taken 8 at a time is approximately 10^{20}; however the size increases dramatically if M increases.

Thus, the DPP is a case in which mathematical expertise is beneficial to formulating the design optimization problem. For example, reference 8 discusses the solution of equation (4) as a mixed ILP problem. The branch and bound algorithm using linear programming relaxations is demonstrated. Topological constraints (e.g., a restriction on the selection of adjacent locations) are quite easy to add. Furthermore, the efficiency of the branch and bound algorithm is sensitive to the number of modes and the number of possible locations (i.e., the dimension of the v matrix) but not to the number of active struts.

The solution to the DPP using branch and bound algorithm surprised both the engineers and the mathematicians. Figure 4 illustrates one solution to equation (4) for selecting locations of eight active struts. This solution was surprising from an engineering standpoint because two locations were selected on the suspension arms near the place

where the cables were attached to the structure. Because these arms were designed to be rigid supports for the flexible truss structure, they were considered unlikely locations for active struts. However, further analysis revealed that the v values for these locations were quite large in several modes. These large values of predicted axial strain energy were partially attributable to a modeling error and led to an improved finite element model for the CEM and a new set of optimal locations. However, the large values were also due to the basic design of the CEM. The next version of the CEM (i.e., Phase 2) had more rigid support arms. Thus, engineering insights gained from solving the mathematical DPP were not only instrumental in finding the best locations for active struts on the Phase 1 CEM but also influenced the design of the Phase 2 CEM.

On the other hand, the experimental results provided important insight to the mathematicians. When active struts were tested in the predicted "optimal" locations they provided little vibration damping for several modes. It was concluded that the method of finding locations using equation (4) has two weaknesses. First, the assumption is made that the structural finite element model is a perfect representation for the CEM. A second assumption asserts that the active struts are identical (i.e., they have the same mass and stiffness properties) to the truss elements they replace. Neither assumption is justified.

An improved version of the DPP would include some uncertainty in specifying the structural finite element model. However, this uncertainty creates mathematical difficulties. For example, if the active struts are significantly different from the truss elements that they replace, then each change in the solution vector x requires a new structural model, a new set of characteristic modes, and a new set of v values. If the number of modes and the values of v are functions of the design variables x then the branch and bound solution to equation (4) becomes impossible and a simulated annealing approach is more appropriate.

The DPP illustrates the need for engineering and mathematical input and the mutual benefits that can be gained in the optimization of engineering systems. However, important questions are raised in regard to the effect of both modeling errors and uncertainty on the optimization process.

Active Structural Acoustic Control (ASAC)

Assume that an aircraft fuselage is represented as a cylinder with rigid end caps (fig. 5) and that a propeller is represented as a point monopole with a frequency equal to some multiple of the blade passage frequency. Piezoelectric (PZT) actuators bonded to the

fuselage skin are represented as line force distributions in the x and θ directions. Using this simplified model, the point monopole produces predictable pressure waves that are exterior to the cylinder. These periodic pressure changes cause predictable structural vibrations in the cylinder wall and predictable noise levels in the interior space. The interior noise level at any discrete microphone location can be dramatically reduced by using the PZT actuators to modify the vibration of the cylinder. For a given set of microphones and a given set of actuator locations, the control forces that minimize the L_2 norm of the noise are known. However, methods for choosing the optimal locations for the microphones and the optimal locations for the actuators have not been considered.

The use of active structural acoustic control in cylindrical fuselage structures is explained in reference 10 and verified by numerous experiments (e.g., refs. 10-12). The results in reference 10 demonstrate that the amount of noise control depends both on the geometry of the source plus the cylinder system and on the locations of discrete control and measuring points. The force limitations of the PZT actuators must be considered in planning the control strategy. In addition, effective noise control strategies can either reduce the vibration of the cylinder or can increase the vibration of the cylinder, which shifts the energy to shell modes that do not couple efficiently with acoustic modes. This insight is important because aircraft manufacturers may reject a noise control method that increases vibration and in turn increases fatigue of the airframe.

In accordance with the notation given in reference 11, the ASAC optimization problem is to minimize the sum of squared pressures at a discrete set of interior microphones:

$$E = \sum_{m=1}^{Np} \Lambda_m \Lambda_m^* \tag{7}$$

where Np is the number of microphones and * indicates the complex conjugate. The response at microphone m is given as:

$$\Lambda_m = \sum_{k=1}^{Nc} H_{mk} c_k + p_m \tag{8}$$

where p_m is the response with no active control and H_{mk} is a complex-valued transfer matrix that represents the pressure at microphone m due to a unit control force ($|c_k| = 1$) at the PZT actuator k. The values in the transfer matrix can be collected experimentally (ref. 11) or they can be simulated (ref. 10).

The cost function can be written as in equation (7) or expressed on a decibel scale which compares the interior pressure norm with and without ASAC:

$$\text{Level} = 10 \log\left(\frac{\sum_{m=1}^{Np} \Lambda_m \Lambda_m^*}{\sum_{m=1}^{Np} P_m P_m^*} \right) \tag{9}$$

Thus, a negative noise level signifies a decrease in the noise due to the action of PZT actuators.

For a fixed set of Nc actuators, the forces c_k which minimize either equation (7) or equation (9) can be determined by solving a complex least-squares problem (ref. 10). Unfortunately, the solution vector may contain values of c_k that exceed the maximum allowable control force. Also, the solution vector may decrease the interior noise level and increase the shell vibration level. (Note that an equation similar to equation (9) exists that compares the vibration norm with and without ASAC. A positive vibration level signifies an increase in shell vibration due to the action of PZT actuators.)

In the ASAC case, engineering input complicated the optimization process. The engineering approach assumed that the forces c_k were variable but that the actuator locations were fixed. Several attempts were made to use multiobjective optimization to trade off noise reduction and vibration reduction while imposing force constraints. These attempts met with limited success (ref. 11). The weakness of this method is that it is a multiobjective formulation and, thus is highly sensitive to the weights placed on each objective.

An alternate way to pose the problem is to make the control forces dependent variables and choose the number and the locations of the actuators. Given a large number Nc of possible locations, the alternate procedure uses tabu search or simulated annealing to converge to the best subset of these locations. As each proposed subset is considered, the vector of control forces that minimizes E (eq. (7)) is calculated and the corresponding noise level (eq. (9)) is used to determine the value of the proposed move.

For many numerical experiments with differing numbers of possible locations, subset sizes, source frequencies and sets of interior microphones, the same trends are observed. Namely, the subset of actuators that reduces interior noise also reduces cylinder vibration. Figure 6 shows typical results. In the figure, noise and vibration levels are plotted versus the tabu search iteration number. The 16 best locations are chosen from a set of 102 possible locations. Notice that the initial set of 16 actuators reduces the noise by 13 dB but increases the cylinder vibration by 4 dB. However, after several iterations, both noise and vibration levels are reduced dramatically. By adjusting the number of actuators up or down from 16, the noise-reduction goals can be satisfied without an increase in vibration and without exceeding force capacity of the PZT actuators.

9

The best locations for PZT actuators are not intuitively obvious. For example, figure 7 shows the grid of 102 possible locations distributed in 6 rings of 17 locations. Each actuator location is specified by the $(x, \theta, r=a)$ position of its center. (Recall fig. 5.)

The acoustic monopole is located at $(x=L/2, \theta=0, r=1.2a)$ where L is the cylinder length and a is the cylinder radius. (The dimensions of the cylinder and the frequency of the source are chosen to simulate typical blade passage frequencies on commuter aircraft.) The shaded rectangles indicate the 16 best actuator locations. Figure 7(a) shows the best locations for controlling interior noise due to an acoustic monopole with a frequency of 200 Hz. Figure 7(b) indicates the change in the best locations for an acoustic monopole with a frequency of 275 Hz. Notice the symmetric pattern in figure 7(a) which corresponds to a case in which the acoustic monopole excites one dominant interior cavity mode. Notice the greater complexity of the pattern in figure 7(b). Here, several cavity modes of similar importance are excited by the 275 Hz. monopole.

The results in figures 6 and 7 are preliminary and are based on simulated transfer matrices. However, they indicate the importance of actuator location in active structural acoustic control. Experimental tests of the actuator placement procedure are planned. In these tests, the transfer matrix will be constructed using measured data and the optimal locations will be verified experimentally.

Concluding Remarks

This paper details the complicated process by which engineering design optimization problems are formulated and solved. Occasionally, as with the antenna assembly-sequence optimization, an engineering description of a problem leads directly to a convenient solution method. More often, with engineering input alone, a multiobjective problem is described for which neither the important design variables nor the appropriate weighting of objectives are obvious. In addition, the design optimization problem is often simulated by a computer code that inadequately models the physical behavior of the system. These shortcomings lead to elegant mathematical solutions but meaningless optimization results.

This paper illustrates the benefits of a synergistic relationship between engineering and mathematical experts. Mathematical expertise can be used to pose a design optimization problem in a less ambiguous manner. Often, mathematical experiments reveal useful trends that were previously unsuspected or uncover weaknesses and coding errors in the analysis codes. The reverse is also true; unexpected optimization results and experimental results can be used to improve mathematical models and to revise an optimization problem.

NASA Langley Research Center

Hampton, VA 23681-0001

October 5, 1995

References

1. Glover, F.: Tabu Search, Part I. *ORSA J. on Computing*, vol. 1, 1989, pp. 190–206.

2. Glover, F.: Tabu Search: A Tutorial. *INTERFACES*, vol. 20, 1990, pp. 74–94.

3. Kincaid, R. K.; and Barger, R. T.: The Damper Placement Problem on Space Truss Structures. *Location Science*, vol. 1, 1993, pp. 219–234.

4. Nemhauser, George L.; and Wolsey, Laurence A.: *Integer and Combinatorial Optimization*, John Wiley & Sons, Inc., 1988, pp. 355–365.

5. Green, W. H.; and Haftka, R. T.: *Reducing Distortion and Internal Forces in Truss Structures by Member Exchange.* NASA TM-101535, 1989.

6. Kincaid, R. K.: Minimizing Distortion and Internal Forces in Truss Structures via Simulated Annealing. *Struct. Optim.*, vol. 4, March 1992, pp. 55–61.

7. Kincaid, Rex K.; *Minimizing Distortion in Truss Structures: A Comparison of simulated annealing and tabu search,* AIAA-91-1095-CP, 1991.

8. Padula, S. L.; and Sandridge, C. A.: Passive/Active Strut Placement by Integer Programming. *Topology Design of Structures.* Martin P. Bendsoe, and Carlos A. Mota Soares, eds., Kluwer Academic Publishers, 1993, pp. 145–156.

9. Chen, G.-S.; Bruno, R. J.; and Salama, M.: Optimal Placement of Active/Passive Members in Structures using simulated annealing. *AIAA J,* vol. 29, no. 8, Aug. 1991, pp. 1327–1334.

10. Silcox, Richard J.; Fuller, Chris R.; and Lester, Harold C.: Mechanisms of Active Control in Cylindrical Fuselage Structures. *AIAA J.,* vol. 28, no. 8, Aug. 1990, pp. 1397–1404.

11. Cabell, R. H.; Lester, H. C.; Mathur, G. P.; and Tran, B. N.: *Optimization of Actuator Arrays for Aircraft Interior Noise Control.* AIAA-93-4447, 1993.

12. Lyle, Karen H.; and Silcox, Richard J.: *A Study of Active Trim Panels for Noise Reduction in an Aircraft Fuselage.* Presented at the General, Corporate and Regional Aviation Meeting and Exposition, Wichita, KS, May 3-5, 1995. SAE paper 95-1179.

Figures

(a) Antenna configuration
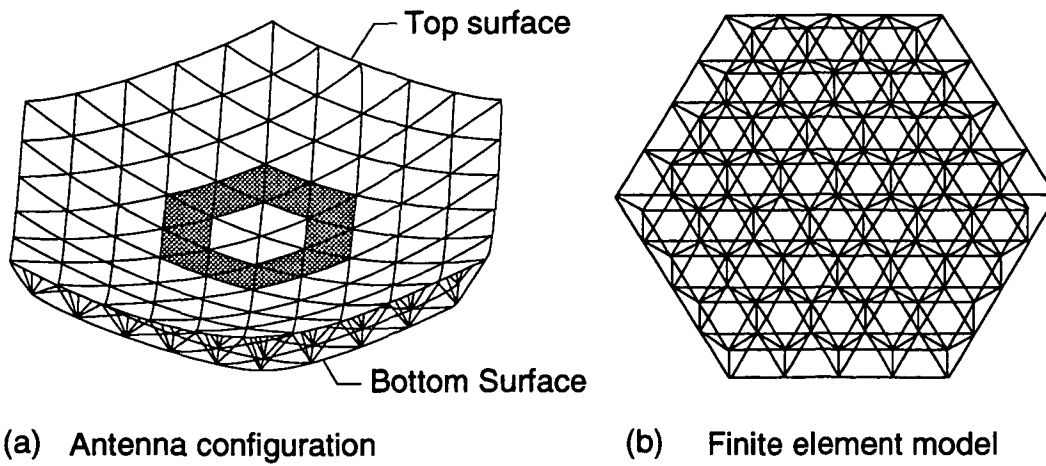
(b) Finite element model

Figure 1. Conceptual design of a large space antenna.
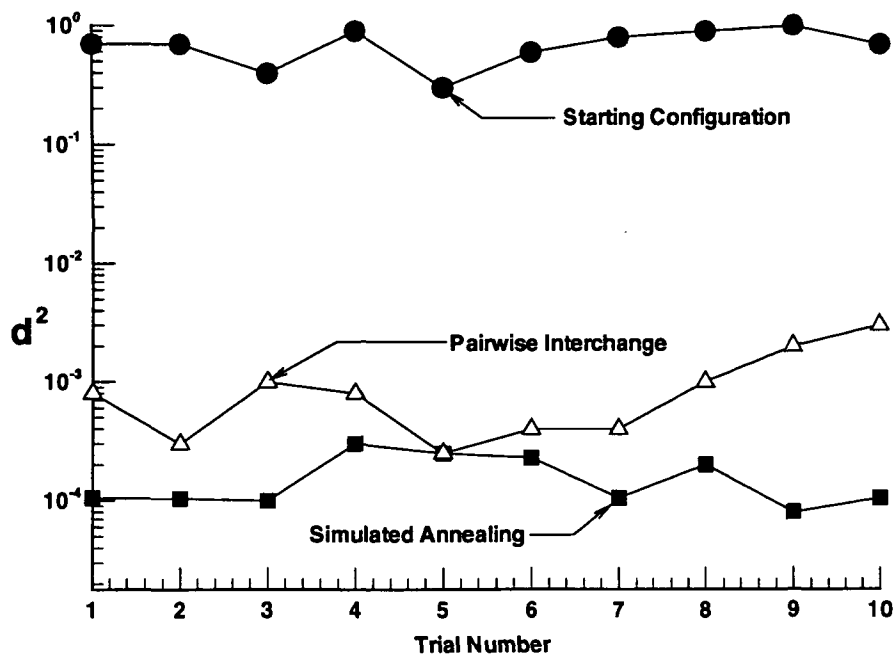

Figure 2. Comparison of solutions found by simulated annealing and pairwise interchange heuristics.
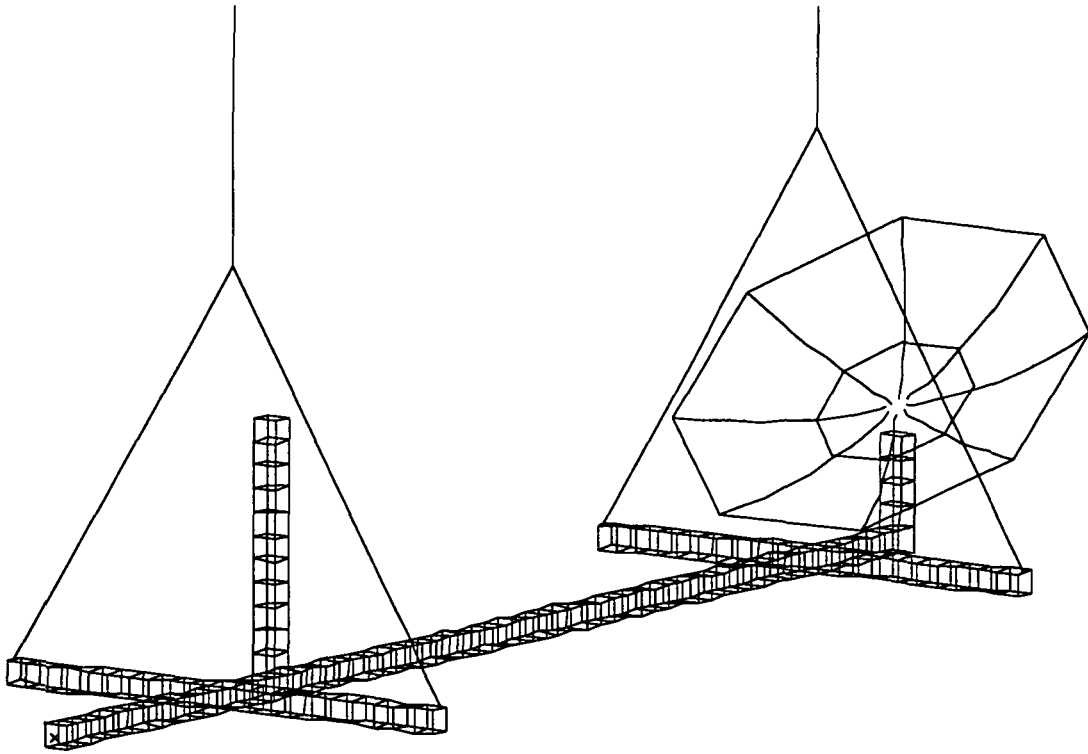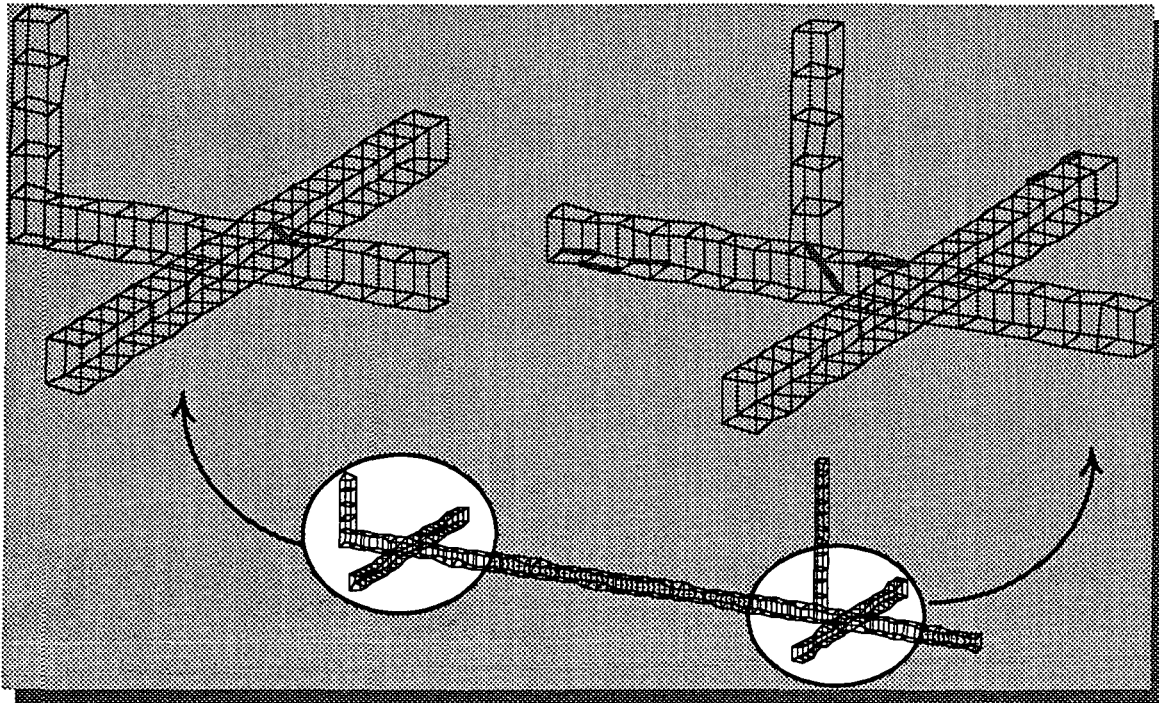
Figure 3. CSI evolutionary model (CEM).

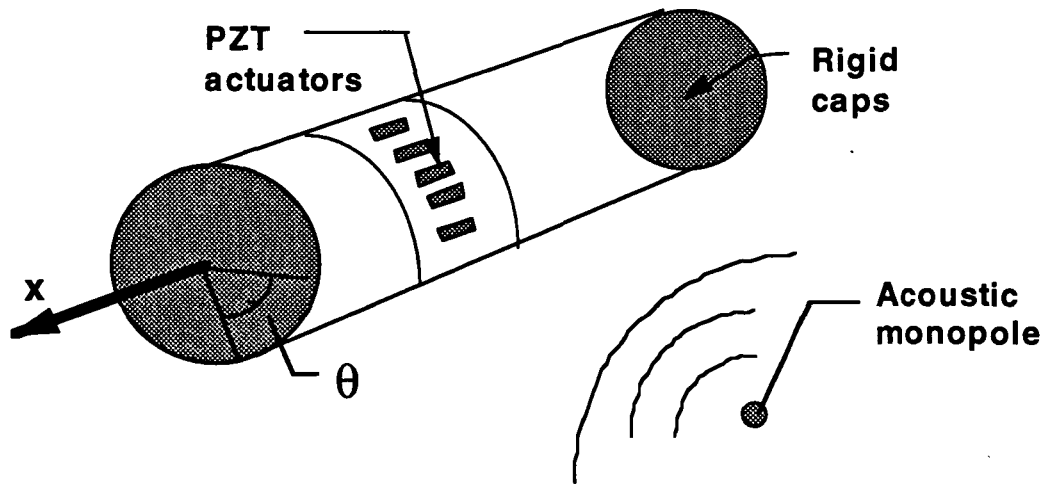Figure 4. Optimal locations for eight active struts on CEM.

14

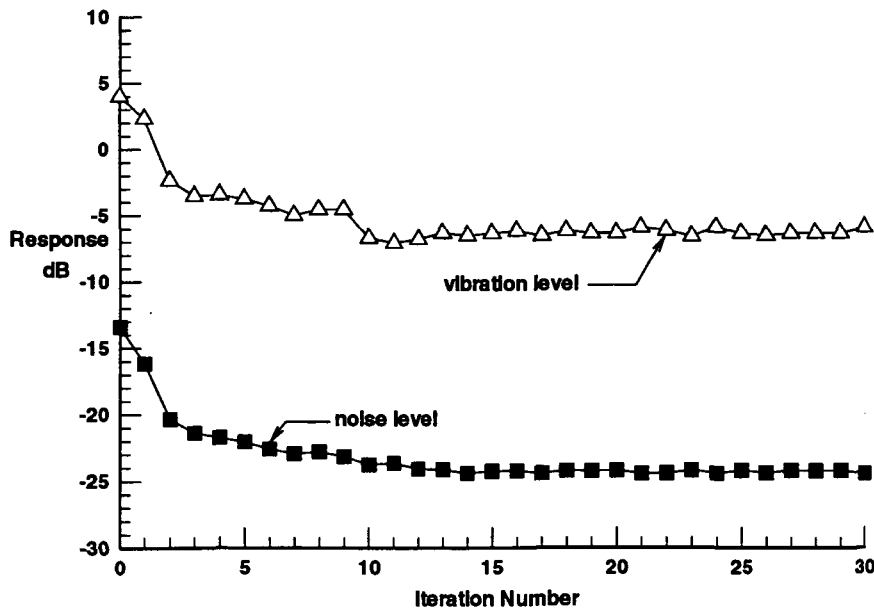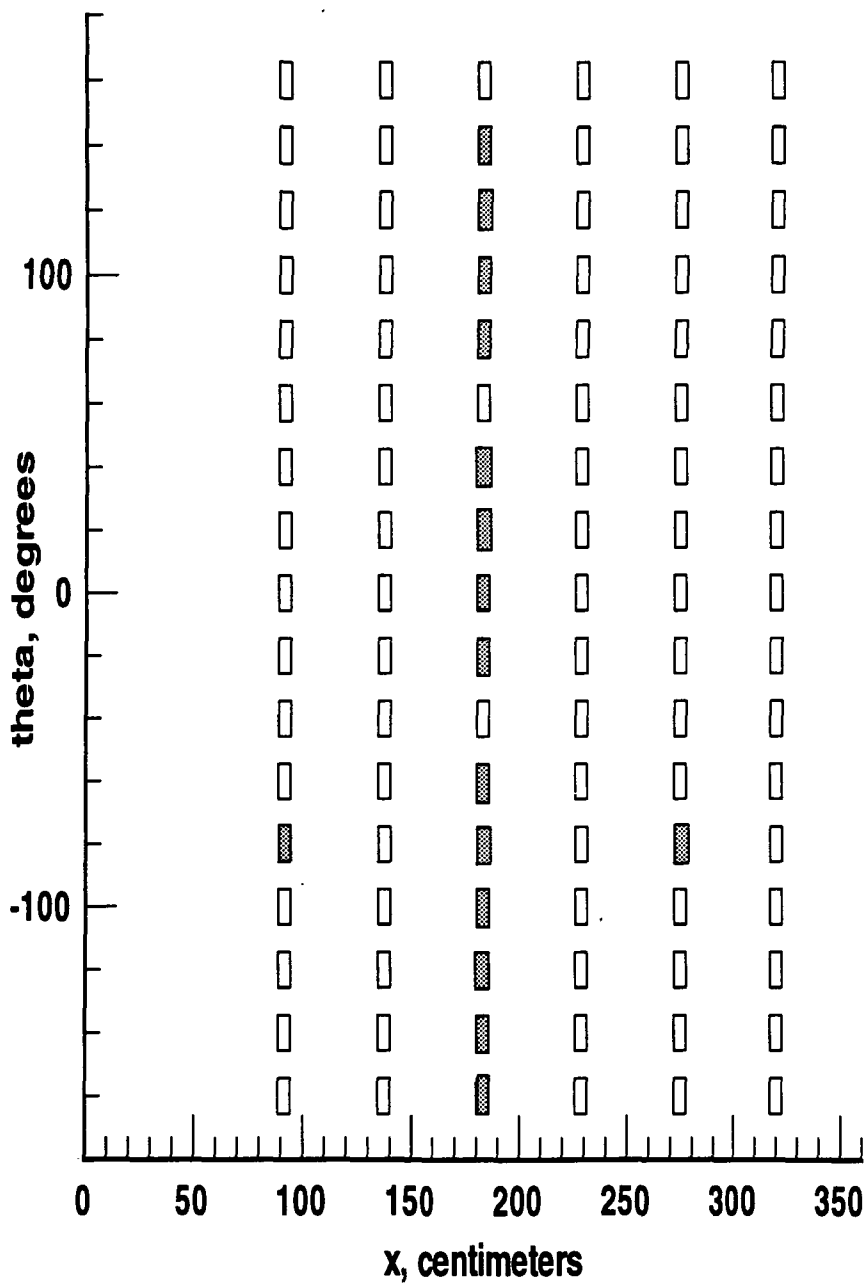Figure 5. Schematic of cylinder and piezoelectric actuators.
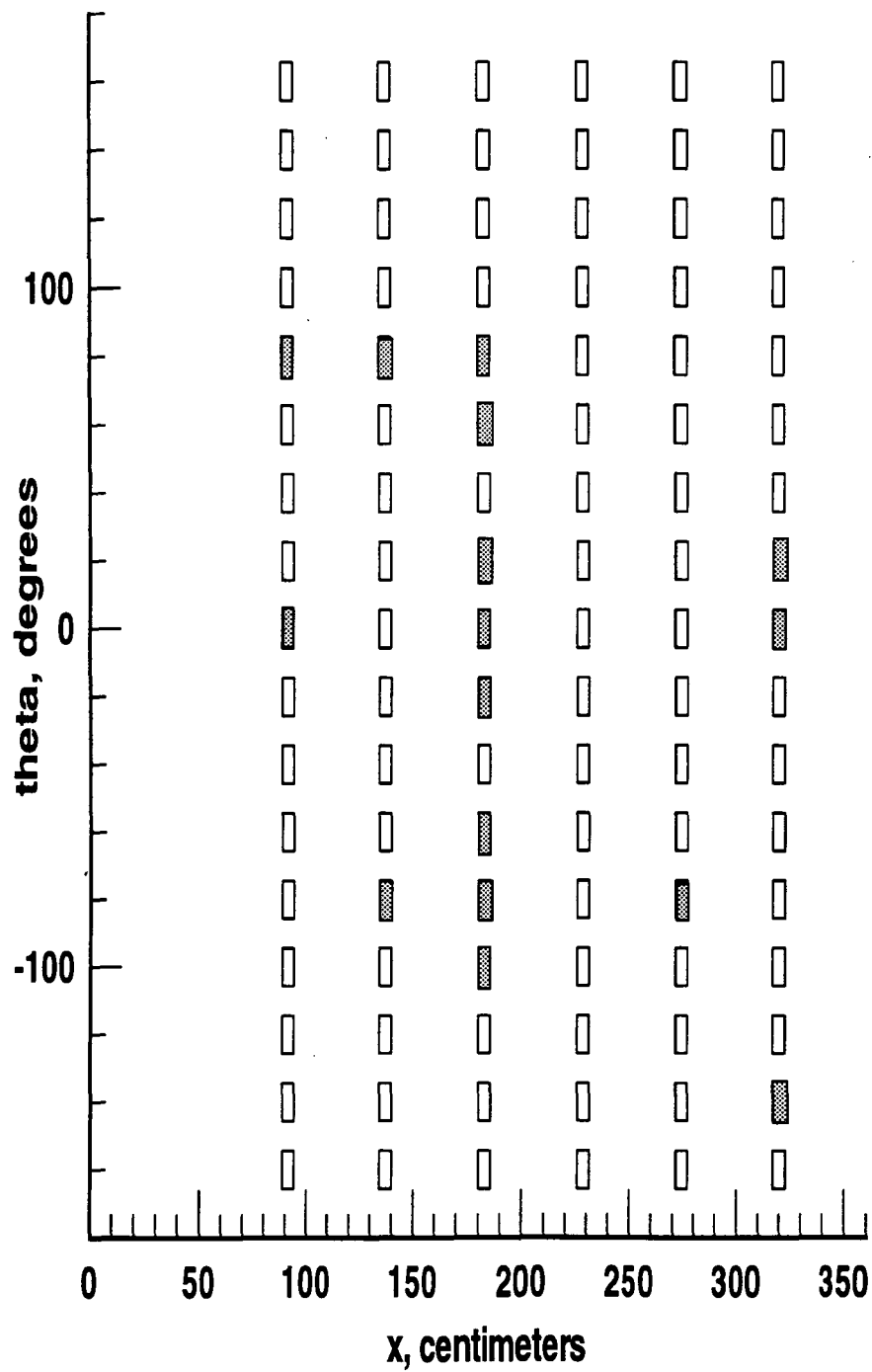

Figure 6. Typical performance of tabu search, which shows simultaneous reduction of noise and vibration.

(a) Frequency = 200 Hz.

Figure 7. Optimal locations for 16 piezoelectric (PZT) actuators on cylinder.

(b) Frequency = 275 Hz.

Figure 7. Concluded.